Estimation of glacier runoff and future trends in the Yangtze River source region, China

LIU Shiyin,[1] ZHANG Yong,[1,2] ZHANG Yingsong,[1] DING Yongjian[1]

[1]*State Key Laboratory of Cryospheric Sciences, Cold and Arid Regions Environmental and Engineering Research Institute, Chinese Academy of Sciences, Lanzhou 730000, China*
E-mail: liusy@lzb.ac.cn
[2]*Graduate School of Environmental Studies, Nagoya University, Nagoya 464-8602, Japan*

ABSTRACT. Glacier runoff from the Yangtze River source region (YRSR), China, is estimated for the period 1961–2000 using a degree-day approach. In the investigation area, glacier runoff accounts for 11.0% of the total river runoff during the period 1961–2000. In the 1990s its contribution to river runoff rises to 17.0%. Due to the current rate of glacier decline, the impact of glacier runoff on river runoff has recently increased in the source region. Based on two different climate-change scenarios derived from ECHAM5/MPI-OM, future glacier runoff is assessed for the period 2001–50. In all climate-change scenarios, annual glacier runoff shows a significant increase due to intensified ice melting. There is an increase in glacier runoff during spring and early summer, yet a significant decrease in late summer. This study highlights the current and future impact of glacier runoff on river runoff in the YRSR.

INTRODUCTION

Worldwide, glaciers have generally experienced retreat and thinning since the beginning of the 20th century (Solomon and others, 2007). Reductions in glacier area and volume have considerable impact on the seasonal and interannual variability of runoff in river catchments because glaciers temporarily store water as snow and ice on many different timescales (e.g. Braun and others, 2000; Jansson and others, 2003). These impacts affect not only the local catchment area but also adjacent lowlands far beyond the limits of the glacierized mountain ranges (Jansson and others, 2003). For this reason, it is important to assess the impact of glacier runoff variability resulting from climate change on river runoff for regional water supplies globally, including in arid and semi-arid regions, and to predict future variability in order to be prepared for new environmental situations.

The Yangtze River source region (YRSR), western China, is the area most sensitive to global warming within the Tibetan Plateau (Kang and others, 2007; Yang and others, 2007). The rate of warming of the YRSR archived in the Geladandong mountain ice core since the 1970s is almost four times higher than the rate of global warming over the past 50 years (0.50 vs 0.13°C (10 a)$^{-1}$) (Kang and others, 2007; Solomon and others, 2007). During recent decades glaciers have shown a rapid retreat in different regions of the YRSR (Ding and others, 1992; Fujita and Ageta, 2000; Lu and others, 2002; Ye and others, 2006). With rapid warming and glacier retreat, a key scientific issue of concern is how variations in glacier runoff will impact on regional water resources and what the trend will be over the coming decades. Runoff from glacier melt is essential to support intense human activity and ecological environmental development in the YRSR. The YRSR is not only an important source of river runoff, it is also the source of fresh water for the daily life of the local native people and alpine wildlife. However, little is known about the variability of glacier runoff and its impact on water resources and the ecological environment of the YRSR. Consequently, a quantitative understanding of potential climate-mediated glacier runoff variability in the YRSR is needed. The objective of this research is to use streamflow simulation modelling to quantify the potential impacts of glacier runoff and to assess future trends in water resources of the YRSR.

STUDY AREA

The YRSR (32°30′–35°35′ N, 90°43′–96°45′ E) is located in the central east part of the Tibetan Plateau (Fig. 1). It has five tributary water systems, the Tuotuo, Dangqu, Qumar, Kouqianqu and Nieqiqu rivers (Fig. 1). The altitude of the YRSR varies from 4200 to 6621 m a.s.l.

Glaciers of the YRSR are primarily distributed on the north slope of the Tanggula mountains, the south slope of the Kunlun mountains and Sedir mountain (Fig. 1). According to the Chinese Glacier Inventory (Shi and others, 2005), there are 753 glaciers in the YRSR, with a total area of 1276 km^2 and a total volume of 100 km^3, accounting for 56.5%, 67.3% and 70.9% of the total number, area and volume, respectively, of all glaciers in the Yangtze River basin (YRB) (Table 1; Shi and others, 2005). The total volume of ice within the YRSR is approximately 887.5×10^8 m^3 w.e., five times the annual discharge of the Zhimenda hydrological station shown in Figure 1 (Shi and others, 2005). Observational data within the YRSR over our study period exist only for the Dongkemadi glacier catchment (Fujita and others, 1996; Zhang and others, 1997; Fujita and Ageta, 2000; Yang, 2006), located in the south of the YRSR (Fig. 1). Its glacierization is approximately 76%, including Da and Xiao Dongkemadi glaciers, where the equilibrium-line altitude (ELA) is ~5600 m a.s.l. (Shi and others, 2005).

DATA

Our study is based on various datasets including daily temperature and precipitation data from national meteorological stations, annual discharge of river runoff from a hydrological station, projected daily temperature and precipitation by ECHAM5/MPI-OM and a digital elevation model (DEM) with a resolution of 90 m.

https://doi.org/10.3189/002214309788608778 Published online by Cambridge University Press

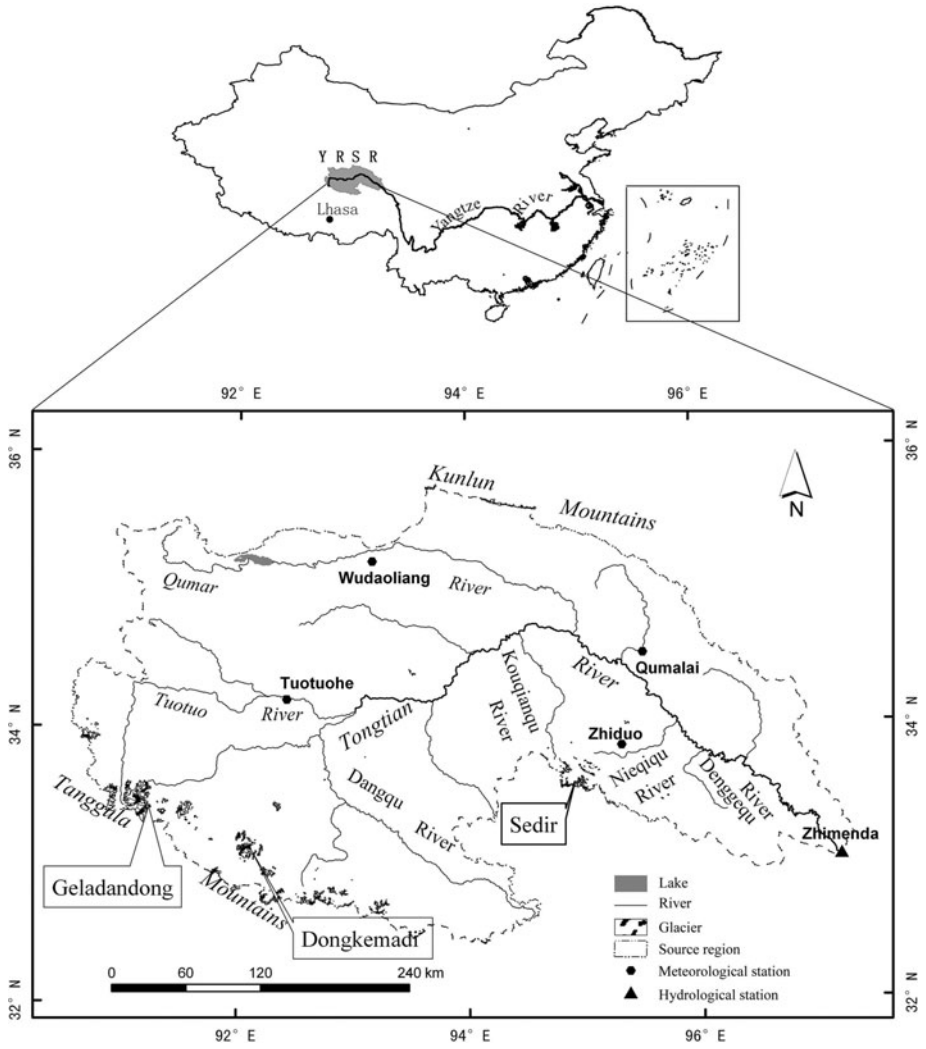

Fig. 1. Location of the Yangtze River source region (YRSR), China, national meteorological stations and hydrological station, and the distribution of glaciers.

Daily temperature and precipitation data are available at four national meteorological stations for the period 1961–2004: Tuotuohe (33.95° N, 92.62° E; 4533 m a.s.l.), Wudaoliang (35.22° N, 93.08° E; 4614 m a.s.l.), Zhiduo (33.85° N, 95.6° E; 4179 m a.s.l.) and Qumalai (34.13° N, 95.78° E; 4176 m a.s.l.) (Fig. 1). Annual discharge of river runoff from the YRSR is available from the Zhimenda hydrological station for the period 1961–2000 (Fig. 1). A DEM with a resolution of 90 m was developed in 1981 based on a digital topographic map with a scale of 1 : 100 000.

Projected daily temperature and precipitation are derived from ECHAM5/MPI-OM, developed at the Max Planck Institute for Meteorology, Hamburg, Germany (Roeckner and others, 2003). Based on the given initial conditions of atmospheric composition before industrialization, ECHAM5/MPI-OM runs with a resolution of $1.875° \times 1.865°$ and with three time-step lengths in the YRB in focus for the period 1941–2050 (Zeng and others, 2007), forced by A2 and B1 emission scenarios from the Intergovernmental Panel on Climate Change (IPCC) Special Report on Emissions Scenarios (SRES) (Solomon and others, 2007). Summary characteristics of A2 and B1 emission scenarios are listed in Table 2. To reduce the uncertainties of a single run of the model, daily data were calculated as the arithmetic mean of the three time-step-length temperatures and precipitations.

Table 1. Glacier population, area and volume for the YRSR and YRB; data derived from the Chinese Glacier Inventory

Site	Number of glaciers		Glacier area		Glacier volume		Average area
		% of YRB	km^2	% of YRB	km^3	% of YRB	km^2
YRSR	753	56.5	1276.06	67.3	100.41	70.9	1.69
YRB	1332		1895		147.26		1.42

https://doi.org/10.3189/002214309788608778 Published online by Cambridge University Press

METHODS

Meteorological data pre-processing

Based on the DEM, the glacierized region of the YRSR is divided, at intervals of 100 m, into a set of elevation bands. Each elevation band is assumed to exhibit different homogeneous hydrological characteristics, and the temperature and precipitation time series are interpolated according to its mean elevation. The interpolation is based on an altitude-dependent regression of the observations at stations located in or near the studied glacierized catchments. For the temperature time series, a constant lapse rate ($0.50^{\circ}C\,(100\,m)^{-1}$) is applied to the temperature series measured at the closest meteorological station (Ding and others, 1992).

The precipitation increases linearly with altitude in the glacierized regions of the YRSR (Ding and others, 1992; Yao, 2002). The precipitation gradient is set to $11.2\%\,(100\,m)^{-1}$ (Zhang and others, 1997; Yao, 2002). Note that the spatial variability of precipitation is high in the glacierized regions of high mountainous catchments, and good spatial interpolation of precipitation data series is therefore difficult to obtain and the prevailing extreme conditions imply significant measurement uncertainty. In addition, the value of the precipitation gradient is difficult to estimate in the glacierized regions of the YRSR where precipitation data are scarce. This difficulty in spatial interpolation of precipitation is a significant source of modelling uncertainty for glacier runoff simulation. Nevertheless, glaciers represent the most important water storage reservoir in the glacierized regions of the YRSR, and for glacier runoff simulation any under- or overestimation of the area-average precipitation can be compensated by simulated ice melt.

Glacier accumulation and melt

For each elevation band, the aggregation state of precipitation is determined according to a simple temperature threshold:

$$\begin{cases} P_{snow} = P_{tot}, & P_{liq} = 0, & T \le T_0 \\ P_{snow} = 0, & P_{liq} = P_{tot}, & T > T_0 \end{cases} \quad (1)$$

where P_{tot} is the total precipitation on a given day, and P_{snow} and P_{liq} are solid and liquid precipitation. T is the mean daily air temperature and T_0 is the threshold temperature.

Correct estimation of the aggregation state of precipitation is essential for the modelling of hydrological processes in high mountain catchments. Although a modelling approach based on a simple threshold function (Equation (1)) does not reflect the observed phenomenon, the results of previous studies have shown that the use of a simple temperature threshold is acceptable for the modelling of hydrological processes in the glacierized regions of high mountain catchments (WMO, 1986; Ye and others, 2004; Zhang and others, 2006c; Hagg and others, 2007). Fortunately, detailed data of precipitation and simultaneous meteorological conditions are available for the four national meteorological stations in the YRSR for the period 1961–79 (Fig. 1). Based on these data, a relationship between the probability of solid precipitation and temperature is obtained (Fig. 2). As indicated in Figure 2, precipitation is almost always solid when the air temperature is below 2.0°C. Above 2.0°C the probability of liquid precipitation significantly increases. This finding is in agreement with previous studies (e.g. Ye and others, 2004; Yang, 2006; Zhang and others, 2006c). We therefore set the value of the threshold parameter to 2.0°C. A mixture of snow and rain is assumed for a transition zone ranging from 1 K above to 1 K below the threshold temperature. Within this temperature range, the snow and rain percentages of total precipitation are obtained from linear interpolation. Redistribution of the original snowfall by wind transport or avalanches is not considered.

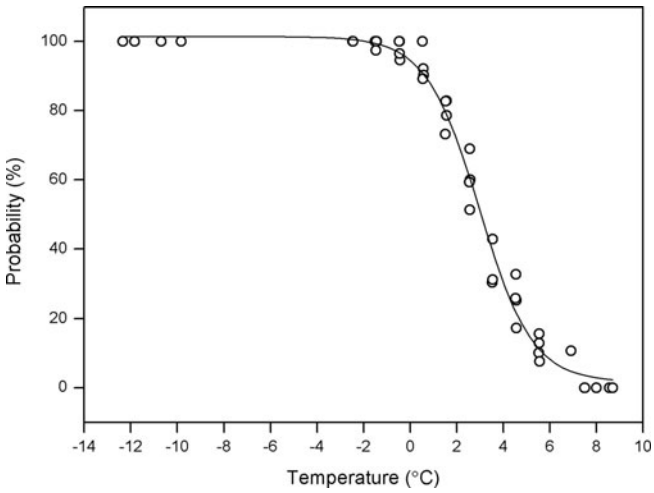

Fig. 2. Relationship between the probability of solid precipitation and temperature in the YRSR.

Glacier melt, M, in the ith elevation band is computed using a degree-day approach, which rests upon a claimed relationship between snow- or ice melt and air temperature, usually expressed in the form of accumulated positive temperatures. Recent work shows that the degree-day approach has been justified more on physical grounds than previously assumed (Ohmura, 2001). Although involving a simplification of complex processes that are more properly evaluated by the energy balance of the glacier surface, the degree-day approach often matches the performance of energy-balance models on the catchment scale (WMO, 1986). Braithwaite and Raper (2002) show that there is excellent consistency between the results of energy-balance models and the degree-day model. The degree-day approach

Table 2. Overview of A2 and B1 emission scenarios from IPCC Special Report on Emissions Scenarios (SRES) (Solomon and others, 2007)

Scenario	Characteristics
A2	A world of independently operating, self-reliant nations; Continuously increasing population; Regionally oriented economic development; Slower and more fragmented technological changes and improvements to per capita income.
B1	Rapid economic growth, but with rapid changes towards a service and information economy; Population rising to 9 billion in 2050 and then declining; Reductions in material intensity and the introduction of clean and resource-efficient technologies; An emphasis on global solutions to economic, social and environmental stability.

https://doi.org/10.3189/002214309788608778 Published online by Cambridge University Press

Table 3. Parameters and their values of the model for the YRSR

Parameter	Value	Unit
Temperature lapse rate	–0.50	°C (100 m)$^{-1}$
Precipitation gradient	11.2	% (100 m)$^{-1}$
Threshold temperature	2.0	°C
Refreezing rate	0.2	–
Degree-day factor for snow	4.1	mm d^{-1} °C^{-1}
Degree-day factor for ice	7.1	mm d^{-1} °C^{-1}

is given by

$$M(i) = \begin{cases} \mathrm{DDF}_{\mathrm{snow/ice}}(T - T_{\mathrm{m}}) & T > T_{\mathrm{m}} \\ 0 & T \le T_{\mathrm{m}} \end{cases} \quad (2)$$

where i is an index for the elevation band, DDF is the degree-day factor, different for snow and ice surfaces, and T_{m} is the threshold temperature for melting, which is set to 0°C.

Glacier runoff

For the entire YRSR, glacier runoff, Q, on a given day is computed as

$$Q = \sum_{i=1}^{n} s(i)\left[(1-f)M(i) + P_{\mathrm{liq}}(i)\right], \quad (3)$$

where $s(i)$ is the area of the ith elevation band, derived from the DEM, and f is the refreezing rate.

Note that since significant amounts of meltwater have been captured as superimposed ice (Fujita and others, 1996), refreezing of meltwater must be taken into account in simulating glacier runoff in the YRSR where cold-type glaciers are dominant (Huang, 1990). Recent work has suggested that approximately 20% of meltwater is preserved at the snow–ice interface due to refreezing processes in the mid- to northern Tibetan plateau (Fujita and others, 2007). Therefore, herein the refreezing rate f is set to 20%.

On the other hand, evaporation is of limited importance in the water balance of the glacierized regions in high mountainous catchments (Braun and others, 1994; Zhang and others, 1997). Previous work has suggested that the estimated annual evaporation from the glacier surface accounts for <6.0% of the total river runoff in the Dongkemadi glacier catchment of the YRSR (Zhang and others, 1997; Yao, 2002). In addition, because the variation of glacier runoff primarily depends on changes of glacier area and climatic conditions, the influence of evaporation from the glacier surface on glacier runoff is small (Ye and others, 1997). It is difficult to estimate evaporation from the glacier surface because of the sparsity of meteorological data in the glacierized regions of the YRSR, and it is not taken into account in the present analyses.

MODEL RESULTS

Model performance assessment

The model has two parameters ($\mathrm{DDF}_{\mathrm{snow}}$ and $\mathrm{DDF}_{\mathrm{ice}}$) to be determined in addition to the above-mentioned fixed model parameters (Table 3). Computations of $\mathrm{DDF}_{\mathrm{ice}}$ and $\mathrm{DDF}_{\mathrm{snow}}$ are based on the available ablation datasets on the north slope of the Tanggula mountains over different periods (Fujita and Ageta, 2000; Yang, 2006). The spatial variability of degree-day factors in western China is analyzed from snow- and ice-melt data and meteorological data from different glaciers (Zhang and others, 2006b). It is found that regional patterns of degree-day factor are detectable and that they vary very little across the Tibetan Plateau (Zhang and others, 2006b). We therefore assume fixed values (Table 3) in the model for these parameters.

Glacier runoff in the glacierized regions of the YRSR is computed from meltwater and rainwater over the period 1961–2000, on the basis of the parameters shown in Table 3. Because few observational data exist in the glacierized regions of the YRSR, it is difficult to assess the performance of the model. The modelling performance is therefore assessed using the following processes.

We use the observed mass balance and ELA of Xiao Dongkemadi glacier to assess the performance of the model. Xiao Dongkemadi glacier is located in the Dongkemadi glacier catchment (Fig. 1), where the mass balance has been measured at a representative set of points in the accumulation area and the ablation area by the stake method once or twice a year since 1988 (Fujita and Ageta, 2000). The annual mass balance at a given point on a glacier is defined as the sum of water accumulation in the form of snow and ice minus the corresponding ablation over the whole year (Paterson, 1994). The above modelling approach enables the estimation of the annual mass balance based on the hydrological simulation outputs. For each elevation band, the mean annual mass balance is calculated based on the simulated snow accumulation and the simulated snow- and ice melt, which is obtained as

$$b_{\mathrm{a},i} = \int_{t_0}^{t_1} \left(P_{\mathrm{snow}}(t) - M_{\mathrm{snow/ice}}(t)\right) \mathrm{d}t, \quad (4)$$

where $b_{\mathrm{a},i}$ is the annual mass balance of the ith elevation band, t_0 is the start date of the measurement year (here 1 October) and t_1 is the end of the measurement year (30 September the following year). The annual mass balance of the entire glacier is estimated as the area-weighted sum of the mass balance of all elevation bands, which is given as

$$B_{\mathrm{a}} = \frac{1}{s_{\mathrm{g}}} \sum_{i=1}^{n} (b_{\mathrm{a},i} s(i)), \quad (5)$$

where B_{a} is the simulated total annual mass balance of the glacier and s_{g} is the area of the entire glacier.

The annual mass balance and ELA of Xiao Dongkemadi glacier were calculated for the period 1988/89–1997/98 using the above approach. As indicated in Figure 3, simulations are in good agreement with observations. Correlation of simulations with observations gives coefficients of 0.93 and 0.88 for the mass balance and ELA of Xiao Dongkemadi glacier respectively, significant at the <1% level. We submit that the processes of glacier ablation and accumulation are sufficiently well simulated by the above modelling approach, which considers only precipitation and temperature as underlying driving forces, and that the applied spatial interpolation of the driving forces can be assumed representative of the glacierized region.

The total ice-volume change in the YRSR for the period 1968–2002 is used to assess the overall performance of the above modelling approach. The volume is estimated using a modified equation suggested by Liu and others (2003):

$$V = 0.04S^{1.35}, \quad (6)$$

where V is the ice volume and S is the total glacier area.

https://doi.org/10.3189/002214309788608778 Published online by Cambridge University Press

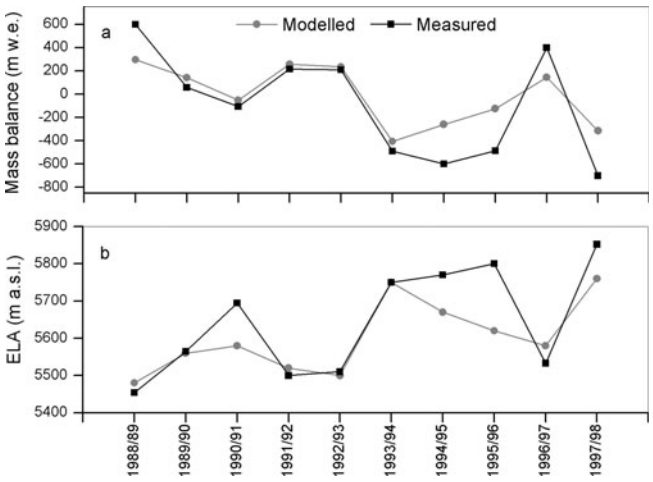

Fig. 3. (a) Measured (squares) and modelled (circles) mean annual mass balance, and (b) the ELA of Xiao Dongkemadi glacier.

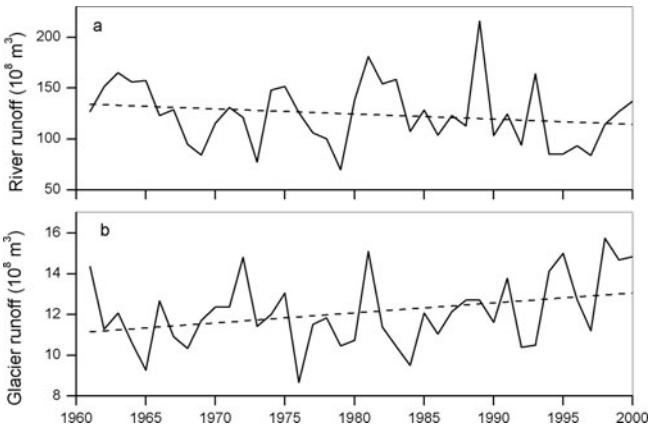

Fig. 4. Variation in annual river runoff (a) and glacier runoff (b) of the YRSR for the climatic normal period 1961–2000. Dashed lines are regression lines indicating trend.

This empirical equation is derived from ice-penetrating radar thickness measurements in different glaciers of western China (Liu and others, 2003), and has been widely applied to estimate glacier volume in different regions of western China (e.g. Liu and others, 2006a,b). The recent glacier changes of the YRSR for the period 1968–2002 were monitored using topographical maps based on aerial photographs acquired during the period 1968–71 and Landsat Enhanced Thematic Mapper Plus (ETM+) images obtained for the period 1999–2002, which indicated that the total glacier area in the YRSR had decreased by approximately 5.3% (Xu and others, in press). On the basis of YRSR glacier area change, the total decrease in YRSR ice volume is estimated from Equation (6) to be $\sim 454.4 \times 10^8$ m^3 w.e. (assuming an ice density of 900 kg m^{-3}). That is, for the period 1968–2002, the water resource in the YRSR increased by approximately 454.4×10^8 m^3 because of the loss of ice mass. Note that the loss of ice volume includes glacier melt and evaporation. Previous studies have suggested that evaporation provides a relatively small contribution to the glacier surface mass loss and is of limited importance to the water balance of the YRSR glacierized regions (Zhang and others, 1997; Yao, 2002). Furthermore, measurements in about 20 evaporation pans showed a gradual decrease in evaporation between 1956 and 2000 (Yang and others, 2007). The evaporation contribution is not separately accounted for within the model. Simulated glacier runoff using the model is approximately 422.0×10^8 m^3 over the entire YRSR for the study period 1968–2002. This agrees closely with the increase in water resources due to ice loss (454.4×10^8 m^3 vs 422.0×10^8 m^3), with a relative error of 7.0%.

Our modelling approach seems to perform well with respect to glacier runoff in the YRSR using the above model parameters, and our results can be regarded as acceptable for the source region where there are no observational glacier runoff data.

Influence of glacier runoff during recent decades

Making use of precipitation and temperature, YRSR glacier runoff is estimated for 1961–2000. For this period, glacier runoff accounts for 11.0% of the total river runoff. As shown in Figure 4b, glacier runoff for the YRSR displayed a generally increasing trend during recent decades, becoming more pronounced in the 1990s. This is associated with an accelerated warming in the 1990s in the YRSR, where the rate of warming estimated from the Geladandong mountain ice core is 0.5°C (10 a)$^{-1}$ since the 1970s, increasing to 1.1°C (10 a)$^{-1}$ during the 1990s (Kang and others, 2007). Various studies have suggested that the response of glacier runoff to climate warming is immediate in the initial phase (Braun and others, 2000; Jansson and others, 2003). With the rapid warming in the 1990s, additional water is released from glacier storage due to intensified melting, resulting in a significant increase in glacier runoff.

Figure 4 shows that, while there was high interannual variability, YRSR river runoff decreased over the period 1961–2000, especially in the 1990s. During this period, river runoff decreased by 13.9%. Glacier runoff increased by 15.2%. As indicated by the decadal anomalies (Fig. 5), river runoff was more plentiful for the periods 1961–70 and 1981–90, while glacier runoff indicated negative anomalies. River runoff in the 1990s reached a minimum, whereas glacier runoff reached a maximum (Fig. 5).

Meteorological data indicate that precipitation in the YRSR significantly increased in winter and spring and dramatically decreased in summer during recent decades (Zhang and others, 2006a; Yang and others, 2007). With rapid warming and decreasing precipitation in summer, the alpine ecosystem, marshland and permafrost are generally degraded and glaciers show rapid retreat (Cheng and Zhao,

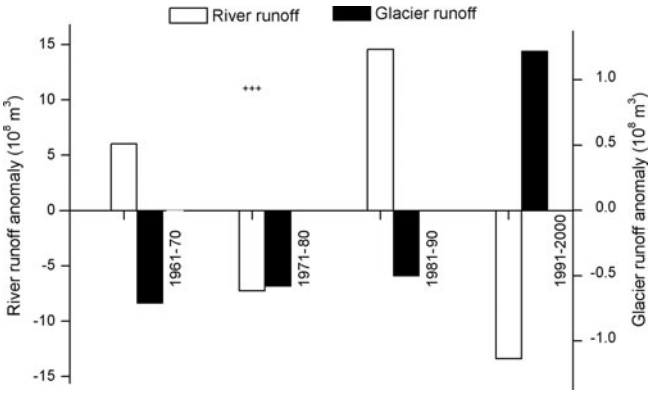

Fig. 5. Decadal river runoff and glacier runoff anomalies for the YRSR during recent decades.

https://doi.org/10.3189/002214309788608778 Published online by Cambridge University Press

Table 4. Parameters of the statistical relationship between the observed and projected data; *r* is correlation coefficient

Scenario	Variable	a_1	a_2	a_3	b	r
A2	*T*	–0.001	0.004	1.2	–1.43	0.92
	P	0.002	–0.07	0.53	0.43	0.50
B1	*T*	–0.001	–0.003	1.2	–1.01	0.92
	P	0.002	–0.06	0.47	0.47	0.50

Table 5. Changes in temperature and precipitation in the YRB and YRSR given A2 and B1 emission scenarios for the period 2001–50, with respect to values for the period 1961–90

Region	Variable	A2	B1	Source
YRB	*T* (°C)	0.22–1.98	0.15–2.04	Zeng and others (2007)
	P (%)	–12.8–6.83	–10.9–13.6	Zeng and others (2007)
YRSR	*T* (°C)	1.44	1.53	This study
	P (%)	–12.2	–10.3	This study

2000; Ye and others, 2006), resulting in significant decrease in river runoff (Ding and others, 2007). Human activity has increased since the end of the 1990s, significantly increasing water demand while the supply decreases, and resulting in intensive degradation of the YRSR alpine ecosystem. Such changes affect not only the source region, but also the middle and lower reaches of the YRB. Glacier runoff in the YRSR, however, rapidly increased during the 1990s, to contribute ~17% of the river runoff. The impact of glacier runoff on river runoff has become stronger than ever before in the YRSR, especially in the 1990s when river runoff exhibited a significant decrease. To a large extent, a significant increase in glacier runoff in the 1990s may have reduced the impact on the YRSR ecological environment of the decrease in river runoff.

FUTURE TRENDS IN GLACIER RUNOFF

YRSR climate scenario

On the basis of ECHAM5/MPI-OM projected temperature and precipitation, possible temperature and precipitation changes in the YRB from 2001 to 2050 were analyzed (Zeng and others, 2007). Compared to the observed temperature and precipitation for the period 1961–2000, the projected temperature and precipitation of ECHAM5/MPI-OM are in good agreement over the entire YRB using the Mann–Kendall test, especially in the upper reaches of the river basin where the performance of ECHAM5/MPI-OM is slightly better than in the middle to lower reaches (Zeng and others, 2007). According to the results of Zeng and others (2007), ECHAM5/MPI-OM is capable of projecting air temperature and precipitation in the YRB, especially for the upper reaches. Nevertheless, meteorological outputs from climate models are not directly applied for impact studies in general, because climate models are unable to represent local subgrid-scale features and dynamics (Giorgi and others, 2001). Biases can develop in both temperature and precipitation, especially precipitation which highly depends on the local orographic conditions. Note that such differences will strongly affect simulated performance since the degree-day approach is particularly sensitive to the seasonal distribution of temperature. Downscaling techniques therefore need to be applied to the climate model output (Wilby and others, 1998; Giorgi and others, 2001).

In this study, we apply a simple statistical downscaling method, a non-linear regression method, which involves establishing a non-linear relationship between a large-scale average surface variable and the local-scale variable (e.g. Kim and others, 1984; Wigley and others, 1990; Wilby and others, 1998). We can build a statistical relationship between the observed and projected climate variables based on the observations of the four meteorological stations in the YRSR. Consequently, future temperature and precipitation time series in A2 and B1 emission scenarios were calculated using

$$y = a_1 x^3 + a_2 x^2 + a_3 x + b, \quad (7)$$

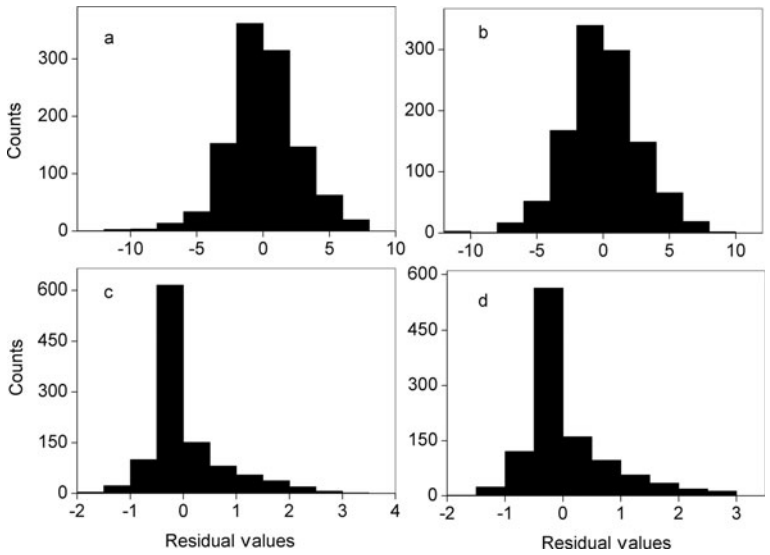

Fig. 6. Histogram of the residuals of (a, b) temperature and (c, d) precipitation in (a, c) A2 and (b, d) B1 emission scenarios.

https://doi.org/10.3189/002214309788608778 Published online by Cambridge University Press

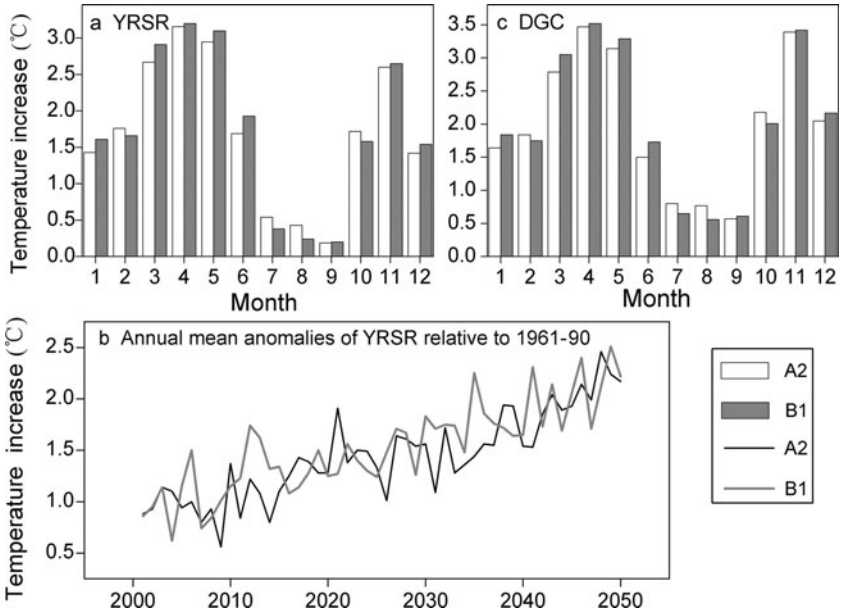

Fig. 7. Variations of temperature projected by ECHAM5/MPI-OM in A2 and B1 emission scenarios in (a, b) the YRSR and (c) the Dongkemadi glacier catchment (DGC) for 2001–50 relative to 1960–90.

where y is a future temperature or precipitation time series, x is a projected temperature and precipitation time series (using ECHAM5/MPI-OM), and a_1, a_2, a_3 and b are parameters given in Table 4. Correlations for precipitation are lower (as expected) than those for temperature (Table 4). This is because the spatial variability of precipitation in the catchment is high, and the reliability of the projected precipitation depends strongly on the local orographic conditions. On the other hand, climate models tend to underestimate large amounts of precipitation and overestimate small amounts (Wilby and others, 1998; Giorgi and others, 2001). The histogram of the residuals indicates that the data are reasonably symmetric, there do not appear to be significant outliers in the tails, and it seems reasonable to assume that the data are from an approximately normal distribution (Fig. 6). It can be seen that the validity of the above downscaling method is acceptable for the present study. According to the above statistical relationship, future temperature and precipitation time series derived from downscaling from ECHAM5/MPI-OM agree closely with the observational data. Correlation coefficients are 0.94 and 0.52, respectively.

As indicated in Table 5, there is a significant increase in temperature in the YRSR, as well as the YRB, in A2 and B1 emission scenarios for the period 2001–50 compared to 1961–90. Surface temperature in the YRSR by 2050 is likely to increase by approximately 1.44°C (A2) and 1.53°C (B1) compared to the climatic normal period (1961–90), especially for spring and winter (Fig. 7a). Precipitation in the source region, however, is likely to reduce by approximately 12.2% and 10.3% (Table 5) in A2 and B1 emission scenarios respectively, compared to the climatic normal period.

Future trend of glacier runoff in the Dongkemadi glacier catchment

The Dongkemadi glacier catchment, situated in the south of the YRSR, is chosen as a representative glacierized region for this study (Fig. 1). Based on the meteorological observations in this catchment, we find an exponential relationship between daily glacier runoff, R_g, and mean daily air temperature, T_g, at 5600 m a.s.l. (Zhang and others, 1997):

$$R_g = 6.8e^{0.222T_g} \ (n = 52,\ r = 0.79). \quad (8)$$

An extensive discussion of this relationship can be found in Zhang and others (1997). As indicated in Figure 7c, future temperature in the Dongkemadi glacier catchment is likely to rise by approximately 1.57°C (A2) and 1.66°C (B1) during 2001–50, with respect to 1961–90, especially in spring and winter. Glacier runoff in the catchment, estimated using Equation (8), is very likely to significantly increase in both A2 and B1 emission scenarios (Fig. 8). Compared to the climatic normal period, glacier runoff by 2050 from this catchment is enhanced by 24.4% (A2) and 25.4% (B1) (Table 6). By 2050, a significant increase in glacier runoff occurs during April–June, with less increase during July–September compared to the climatic normal period (Fig. 8b). In the A2 emission scenario, the depth of glacier runoff varies from 0.06 to 7.8 mm, and from 0.07 to 8.1 mm in the B1 emission scenario. Contemporary comparison shows that the maximum glacier runoff in the B1 emission scenario occurs earlier than in the A2 emission scenario (Fig. 8a). On the other hand, climate warming in this catchment is

Table 6. Glacier runoff during 1961–90 and in A2 and B1 emission scenarios in the Dongkemadi glacier catchment (DGC) and the YRSR

	DGC		YRSR	
	Mean runoff depth	Increase	Mean runoff	Increase
	mm	%	10^8 m^3	%
1961–90	800.8	–	18.0	–
A2	995.8	24.4	23.2	29.2
B1	1004.3	25.4	23.3	29.8

https://doi.org/10.3189/002214309788608778 Published online by Cambridge University Press

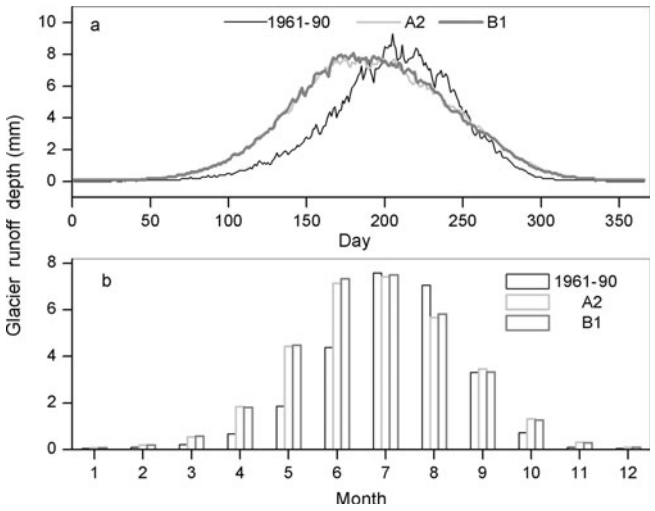

Fig. 8. (a) Daily and (b) monthly variations of glacier runoff for the period 1961–90, in A2 and B1 emission scenarios in the Dongkemadi glacier catchment.

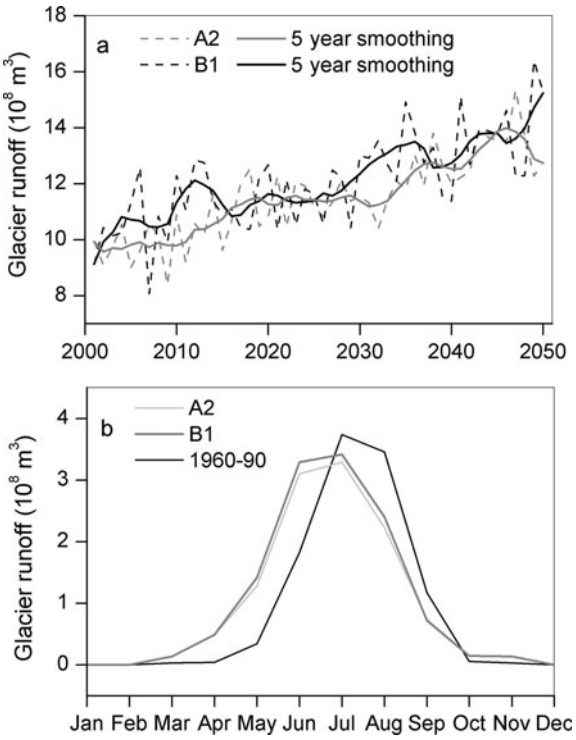

Fig. 9. (a) Evolution of annual glacier runoff in A2 and B1 emission scenarios (2001–50) and (b) annual cycle of glacier runoff (averaged over the period 1960–90), in A2 and B1 emission scenarios in the YRSR.

expected to prolong the glacier melt season (Fig. 8a), thus reducing seasonal runoff concentration, i.e. the ratio of maximum monthly to mean monthly glacier runoff is expected to decrease from 3.5 during the period 1961–90 to 2.7 during the coming half-century in A2 and B1 emission scenarios.

Future trend of glacier runoff in the YRSR

Based on the climate-change scenarios, glacier runoff in the YRSR was estimated for the period 2001–50 using Equations (1–3). The evolution of annual glacier runoff shows a uniform pattern in A2 and B1 emission scenarios for the period 2001–50 (Fig. 9a and b). Discharge gradually increases in the near future due to enhanced melting. Compared to the climatic normal period 1961–90, glacier runoff by 2050 is expected to increase by 29.2% (A2) and 29.8% (B1) (Table 6), i.e. almost twice the increase during the period 1991–2000 when the annual runoff was 15.2% higher than during the climatic normal period.

We have evaluated the annual glacier runoff cycle during the period 1961–90 and in A2 and B1 emission scenarios (Fig. 9c). By 2050, the results of the two emission scenarios show a significant decrease in the July–August runoff to much lower values than during 1961–90: –23.2% (A2) and –19.1% (B1). In contrast, there is a significant increase in the April–June runoff during an earlier onset of the melt season: +121.1% (A2) and +136.0% (B1). Due to enhanced temperature, there is a significant increase in the length of the melt season (Fig. 9c), reducing the seasonal runoff concentration, i.e. the ratio of maximum monthly to mean monthly glacier runoff decreases from 3.0 during the period 1961–90 to 2.2 during 2001–50.

The response of glacier runoff to climate warming is a matter of timescale. Although glacier runoff significantly increases through enhanced meltwater production and more efficient water transport through glaciers in recent decades, it will decrease due to some response variables changing sign at a later stage when enhanced melt rates have caused glacier volume to decrease significantly under a continuous warming in the coming decades (Braun and others, 2000; Jansson and others, 2003). However, glacier runoff in the YRSR by 2050 still shows a significant increase as indicated in Figure 9a and b. It can be seen that the contribution of glacier runoff to river runoff of the YRSR is important during the first half of the 21st century.

DISCUSSION

The shear stress, τ_b, across the base of a column within a glacier is balanced by the equilibrium driving stress, i.e. the component of the weight of the column parallel to the glacier surface (Paterson, 1994). Thus

$$\tau_b = \rho g H \sin\alpha, \tag{9}$$

where ρ is ice density, g is acceleration due to gravity, H is ice thickness and α is the glacier surface slope. If glacier ice is assumed to be a perfect plastic material, Equation (9) can be written as

$$H = \frac{\tau_0}{\rho g \sin\alpha}, \tag{10}$$

where τ_0 is the ice yield stress, with value 100 kPa (Paterson, 1994). Ice thickness may be estimated from the surface slope of a glacier using Equation (10). Such an equation was first applied in central Greenland, and the predicted thickness was consistent with the measured value with a relative error of only about 1.5% (Paterson, 1994). This equation was also reliably applied to estimate the ice thickness (length of an ice core to bedrock) on Malan ice cap, northern Tibetan Plateau (Wang and others, 2006).

The surface slope, α, on glaciers of the YRSR was derived from the DEM with resolution 90 m using Geographic Information System techniques. α varies from 9.1° to 13.2°. Consequently, assuming α to be constant during

https://doi.org/10.3189/002214309788608778 Published online by Cambridge University Press

2001–50, variations in ice thickness at different elevation bands of the YRSR were estimated according to Equation (10). Combined with glacier melt rates in different elevation bands estimated from Equation (2), it is found that glaciers of the YRSR can be expected to experience noticeable thinning in A2 and B1 emission scenarios by 2050. For example, glacier ice may disappear from the areas below 5500 m a.s.l. in the Tuotuo river basin, where the lowest glacier terminus elevation is about 5120 m a.s.l. Glacier shrinkage is more significant in the B1 emission scenario than in the A2 scenario. On average, glacier termini throughout the YRSR are likely to retreat to ~5490 m a.s.l., given the B1 emission scenario, by 2050. On the basis of the total glacier meltwater calculated from Equation (2) for 2001–05, the area and volume of glaciers in the YRSR were estimated by Equation (6). These are likely to reduce by approximately 8.4% and 11.1% respectively compared to the total area and volume in the period 1999–2002.

CONCLUSIONS

In the YRSR, glacier runoff has a dominant impact on the seasonal and interannual variability of river runoff. For recent decades, we have estimated glacier runoff using the degree-day approach, accounting for 11.0% of the total river runoff in the YRSR. In particular, glacier runoff exhibits a significant increasing trend with a rapid increment in the 1990s, and its contribution amounts to 17.0% of the total river runoff. Glacier runoff is an important contributor to the water resources of the YRSR, especially considering the decreasing trend in streamflow during recent decades.

For the period 2001–05, glacier runoff in the YRSR is likely to significantly increase in A2 and B1 emission scenarios projected by ECHAM5/MPI-OM. For the Dongkemadi glacier catchment, glacier runoff is expected to increase by 24.4% and 25.4% in A2 and B1 emission scenarios respectively, with respect to the average value for 1961–90, i.e. 29.2% and 29.8% of the entire YRSR. We predict a significant decrease in glacier runoff during the summer months, yet an increase in spring. The results indicate that substantial changes will occur in the glacier runoff regime of the YRSR, linked with climate change. These changes will have an impact over coming decades on the management, on both the local and regional scale, of the water resources of the YRSR.

ACKNOWLEDGEMENTS

This research was supported by the Key Research Project of the Knowledge Innovation Project of the Chinese Academy of Sciences (CAS) (grant No. Kzcx2-yw-301), the National Essential Scientific Program of the Ministry of Science and Technology of the People's Republic of China (grant No. 2006FY110200) and the National Natural Science Foundation of China (grant No. 40701032, No. 40571034 and No. 40371026). We thank Tong Jiang of the Nanjing Institute of Geography and Limnology of the CAS, for providing the projected data of ECHAM5/MPI-OM. We are grateful to the National Climate Center, China Meteorological Administration, for meteorological data at stations in the YRSR. We also thank two anonymous reviewers and the scientific editor B. Kulessa for helpful comments and suggestions.

REFERENCES

Braithwaite, R.J. and S.C.B. Raper. 2002. Glaciers and their contribution to sea level change. *Phys. Chem. Earth,* **27**(32–34), 1445–1454.

Braun, L.N. *and 7 others*. 1994. Measurement and simulation of high Alpine water balance components in the Linth-Limmern head watershed (north-eastern Switzerland). *Z. Gletscherkd. Glazialgeol.,* **30**, 161–185.

Braun, L.N., M. Weber and M. Schulz. 2000. Consequences of climate change for runoff from Alpine regions. *Ann. Glaciol.,* **31**, 19–25.

Cheng, G. and L. Zhao. 2000. The problems associated with permafrost in the development of the Qinghai–Xizang Plateau. *Quat. Sci.,* **20**(6), 521–531. [In Chinese.]

Ding, Y., Z. Li, S. Liu and X. Yu. 1992. Glacioclimatological features in the Tanggula Mountains, China. *Ann. Glaciol.,* **16**, 1–6.

Ding, Y., B. Ye, T. Han, Y. Shen and S. Liu. 2007. Regional difference of annual precipitation and discharge variation over west China during the last 50 years. *Sci. China D,* **50**(6), 936–945.

Fujita, K. and Y. Ageta. 2000. Effect of summer accumulation on glacier mass balance on the Tibetan Plateau revealed by mass-balance model. *J. Glaciol.,* **46**(153), 244–252.

Fujita, K., K. Seko, Y. Ageta, J. Pu and T. Yao. 1996. Superimposed ice in glacier mass balance on the Tibetan Plateau. *J. Glaciol.,* **42**(142), 454–460.

Fujita, K., T. Ohta and Y. Ageta. 2007. Characteristics and climatic sensitivities of runoff from a cold-type glacier on the Tibetan Plateau. *Hydrol. Process.,* **21**(21), 2882–2891.

Giorgi, F. *and 9 others*. 2001. Regional climate information: evaluation and projections. In Houghton, J.T. *and 7 others, eds. Climate change 2001: the scientific basis. Contribution of Working Group I to the Third Assessment Report of the Intergovernmental Panel on Climate Change*. Cambridge, etc., Cambridge University Press, 583–638.

Hagg, W., L.N. Braun, M. Kuhn and T.I. Nesgaard. 2007. Modelling of hydrological response to climate change in glacierized Central Asian catchments. *J. Hydrol.,* **332**(1–2), 40–53.

Huang, M. 1990. On the temperature distribution of glaciers in China. *J. Glaciol.,* **36**(123), 210–216.

Jansson, P., R. Hock and T. Schneider. 2003. The concept of glacier storage: a review. *J. Hydrol.,* **282**(1–4), 116–129.

Kang, S. *and 6 others*. 2007. Recent temperature increase recorded in an ice core in the source region of Yangtze River. *Chinese Sci. Bull.,* **52**(6), 825–831.

Kim, J.-W., J.-T. Chang, N.L. Baker, D.S. Wilks and W.L. Gates. 1984. The statistical problem of climate inversion: determination of the relationship between local and large-scale climate. *Mon. Weather Rev.,* **112**(10), 2069–2077.

Liu, S., W. Sun, Y. Shen and G. Li. 2003. Glacier changes since the Little Ice Age maximum in the western Qilian Shan, northwest China, and consequences of glacier runoff for water supply. *J. Glaciol.,* **49**(164), 117–124.

Liu, S. *and 8 others*. 2006a. Glacier changes during the past century in the Gangrigabu mountains, southeast Qinghai–Xizang (Tibetan) Plateau, China. *Ann. Glaciol.,* **43**, 187–193.

Liu, S. *and 7 others*. 2006b. Glacier retreat as a result of climate warming and increased precipitation in the Tarim river basin, northwest China. *Ann. Glaciol.,* **43**, 91–96.

Lu, A., T. Yao, S. Liu, L. Ding and G. Li. 2002. Glacier change in the Geladandong area of the Tibetan Plateau monitored by remote sensing. *J. Glaciol. Geocryol.,* **24**(5), 559–562.

Ohmura, A. 2001. Physical basis for the temperature-based melt-index method. *J. Appl. Meteorol.,* **40**(4), 753–761.

Paterson, W.S.B. 1994. *The physics of glaciers. Third edition.* Oxford, etc., Elsevier.

Roeckner, E. *and 13 others*. 2003. The atmospheric general circulation model ECHAM5. Part I: model description. *Max-Planck-Inst. Meteorol. Rep.* 349.

https://doi.org/10.3189/002214309788608778 Published online by Cambridge University Press

Shi, Y., C. Liu, Z. Wang, S. Liu and B. Ye, *eds*. 2005. *A concise China glacier inventory.* Shanghai, Shanghai Science Popularization Press. [In Chinese.]

Solomon, S. *and 7 others, eds*. 2007. *Climate change 2007: the physical science basis. Contribution of Working Group I to the Fourth Assessment Report of the Intergovernmental Panel on Climate Change*. Cambridge, etc., Cambridge University Press.

Wang, N., T. Yao, J. Pu, Y. Zhang and W. Sun. 2006. Climatic and environmental changes over the last millennium recorded in the Malan ice core from the northern Tibetan Plateau. *Sci. China D,* **49**(10), 1079–1089.

Wigley, T.M.L., P.D. Jones, K.R. Briffa and G. Smith. 1990. Obtaining sub-grid-scale information from coarse-resolution general circulation model output. *J. Geophys. Res.,* **95**(D2), 1943–1953.

Wilby, R. *and 6 others*. 1998. Statistical downscaling of general circulation model output: a comparison of methods. *Water Resour. Res.,* **34**(11), 2995–3008.

World Meteorological Organization (WMO). 1986. Intercomparison of models of snowmelt run-off. *WMO Rep*. 646. (Operational Hydrology Report No. 23.)

Xu, J., S. Liu, Y. Ding and S. Zhang. In press. Glacier changes over the past three decades in the Yangtze river source region. *Acta Geogr. Sin*. [In Chinese with English summary.]

Yang, J. 2006. Measurement and simulation research on hydrological processes in the source region of the Changjiang and Huanghe Rivers. *In* Yang, J., Y. Ding, R. Chen and J. Liu, *eds*. 2006. *Synthetical study of eco-environmental changes in the source regions of the Changjian and Huanghe Rivers.* Beijing, Meteorological Press, 102–115. [In Chinese.]

Yang, J., Y. Ding and R. Chen. 2007. Climatic causes of ecological and environmental variations in the source regions of the Yangtze and Yellow Rivers of China. *Environ. Geol.,* **53**(1), 113–121.

Yao, T. *ed.* 2002. *Dynamical characteristics of cryosphere in the central section of Qinghai–Tibetan Plateau.* Beijing, Geological Press. [In Chinese with English summary.]

Ye, B., K. Chen and Y. Shi. 1997. Responses of glacier and glacier runoff to climatic change – a model in simulating the Glacier No. 1 in headwaters of the Urumqi River. *Sci. Geogr. Sin.,* **17**(1), 32–40. [In Chinese with English summary.]

Ye, B., D. Yang, Y. Ding, T. Han and K. Toshio. 2004. A bias-corrected precipitation climatology for China. *J. Hydromet.,* **5**(6), 1147–1160.

Ye, Q., S. Kang, F. Chen and J. Wang. 2006. Monitoring glacier variations on Geladandong mountain, central Tibetan Plateau, from 1969 to 2002 using remote-sensing and GIS technologies. *J. Glaciol.,* **52**(179), 537–545.

Zeng, X., B. Su, T. Jiang and J. Wang. 2007. Projection of future climate change in the Yangtze River basin for 2001–2050. *Adv. Climate Change Res.,* **3**(5), 293–298. [In Chinese with English summary.]

Zhang, G., X. Shi, D. Li, Q. Wang and S. Dai. 2006. Climate change in Tuotuohe area at the headwaters of Yangtze River. *J. Glaciol. Geocryol.,* **28**(5), 678–685. [In Chinese with English summary.]

Zhang, Y. *and 7 others*. 1997. The features of hydrological processes in the Dongkemadi River basin, Tanggula Pass, Tibetan Plateau. *J. Glaciol. Geocryol.,* **19**(3), 214–222. [In Chinese with English summary.]

Zhang, Y., S. Liu, C.W. Xie and Y. Ding. 2006a. Observed degree-day factors and their spatial variation on glaciers in western China. *Ann. Glaciol.,* **43**, 301–306.

Zhang, Y., S. Liu, Y. Ding, J. Li and D. Shangguan. 2006b. Preliminary study of mass balance on the Keqicar Baxi Glacier on the south slopes of Tianshan Mountains. *J. Glaciol. Geocryol.,* **28**(4), 477–484. [In Chinese with English summary.]

MS received 28 March 2008 and accepted in revised form 17 October 2008